sustainability

MDPI

Article

Energy Management and Operational Planning of an Ecological Engineering for Carbon Sequestration in Coastal Mariculture Environments in China

Tiancheng Lin [1], Wei Fan [1,*], Canbo Xiao [1], Zhongzhi Yao [1], Zhujun Zhang [1], Ruolan Zhao [1], Yiwen Pan [1] and Ying Chen [1,2]

[1] Ocean College, Zhejiang University, Zhoushan 316000, China; ltc@zju.edu.cn (T.L.); cbxiao@zju.edu.cn (C.X.); 11834006@zju.edu.cn (Z.Y.); zhangzhujun@zju.edu.cn (Z.Z.); 21734124@zju.edu.cn (R.Z.); evelynpan@zju.edu.cn (Y.P.); ychen@zju.edu.cn (Y.C.)

[2] The State Key Lab of Fluid Power and Mechatronic System, Zhejiang University, Hangzhou 310027, China

* Correspondence: wayfan@zju.edu.cn

Received: 22 April 2019; Accepted: 2 June 2019; Published: 5 June 2019

Abstract: China is now accelerating the development of an ecological engineering for carbon sequestration in coastal mariculture environments to cope with climate change. Artificial upwelling as the ecological engineering can mix surface water with bottom water and bring rich nutrients to the euphotic zone, enhance seaweed growth in the oligotrophic sea area, and then increase coastal carbon sequestration. However, one of the major obstacles of the artificial upwelling is the high energy consumption. This study focused on the development of energy management technology for air-lift artificial upwelling by optimizing air injection rate. The fundamental principle underlying this technology is that the mode and intensity of air injection are adjusted from the feedback of information on velocity variation in tidal currents, illumination, and temperature of the surface layer. A series of equations to control air injection was derived based on seaweed growth and solar power generation. Although this finding was originally developed for the air-lift artificial upwelling, it also can be used in other areas of engineering, such as water delivery, aeration, and oxygenation. The simulations show that using a variable air injection rate can lift more nitrogen nutrients of 28.2 mol than using a fixed air injection rate of 26.6 mol, mostly with the same energy cost. Using this control algorithm, the changed temperature and dissolved oxygen profiles prove the effective upwelling in the experiments and the average weights of kelp are 33.1 g in the experimental group and 10.1 g in the control group. The ecological engineering was successfully increasing crop yield for carbon sequestration in coastal mariculture environments.

Keywords: Ecological engineering; Artificial upwelling; Energy management; Mariculture; Carbon sequestration

1. Introduction

China is under tremendous stress to cope with climate change, which is one of the most serious challenges we face for sustainable development of human society [1,2]. The oceans are the largest carbon pool on earth and have the potential of enhancing marine carbon sequestration. Large-scale seaweed aquaculture, as an important approach to counteract the current greenhouse effect and global climate change, has a significant impact on the global carbon cycle [2]. The large-scale seaweed aquaculture can reduce the partial pressure of CO_2 in surface seawater via photosynthesis, which favors diffusion of atmospheric CO_2 into seawater. Later, a portion of the organic carbon would be removed from the water after its seasonal harvest and another portion would sink out of the surface layer into the deep ocean via the biological pump [3]. In addition, seaweed has a great economic

value as food and an energy source [4]. However, large-scale seaweed aquaculture will weaken the hydrodynamic conditions and hinder nutrients supply from entering the upper layer of the water body, resulting in a local oligotrophic state during the seaweed growth season especially. In this situation, nutrient requirements of seaweed growth cannot be met. It is the one of the major factors contributing to the root rot disease and large-scale seaweed dying, which not only reduces the productivity of seaweeds, but may also reverse the contribution of seaweed aquaculture from a strong CO_2 sink to source [5].

Artificial upwelling, which has attracted increasing attention, is considered a promising way to reduce the accumulation of anthropogenic carbon dioxide in the atmosphere and then stimulate the self-healing capacity of the earth [6]. This practice could transport nutrient-rich bottom water to the surface water, enhance seaweed growth, and consequently increase the net inorganic carbon absorption [2,7]. Under the most optimistic assumptions, artificial upwelling is estimated to have the potential to sequester atmospheric CO_2 at rate of approximately 0.9 Pg C/yr [8], which is almost half the CO_2 uptake rate of the global open ocean [9]. Based on related simulations and sea trial experiments, artificial upwelling is considered to have positive effects on increasing primary productivity and enhancing the ability of the ocean to absorb atmospheric CO_2 [10,11]. In addition, using artificial upwelling, the carbon source can be transformed into the carbon sink by adjusting engineering parameters in a specific region and season [12].

According to the differences of drive mode, existing artificial upwelling technology can be divided into five types. First, by building an artificial submarine ridge, we can create upwelling with the influence of current, but it is substantial work and costly. Second, we can use a mechanical pump to lift deep-sea water. The device named "TAKUMI" is an example for artificial upwelling in this manner [13]. It costs a lot of energy and has low efficiency. An artificial upwelling system named Density Current Generator (DCG), developed by the University of Tokyo, has been successfully deployed and tested in Gokasyo Bay (a semi-closed bay), Japan, since 1997. Driven by land-based power supply, the device extracts surface and bottom seawater and mixes them fully before distributing them horizontally into the intermediate layer [14,15]. Using a power of 12 kW, DCG has the ability of discharging 12,000 m^3 of mixed seawater every day. Third, one can use the salinity gradient energy to drive upwelling [16]. Through a long pipe connecting the surface and deep water, the deep water will be lifted continuously once it is given initial motive force. Fourth, create upwelling by wave energy or current [17–19]. K.E. Kenyon proposes a method using a rigid open-ended pipe submerged in the ocean [18]. It is below the surface wave and fixed in the vertical position. Based on Bernoulli's theorem, if wave exists, there is an upwelling because of the different pressure at the head and end of pipe. The last type is air-lift artificial upwelling, which lifts water by the air pump. Zhejiang University and Taiwan University study the air-lift artificial upwelling technology together, which uses air pump and air pipe to produce the upwelling [20,21]. McClimans et al. reported a controlled artificial upwelling by using a bubble curtain in the western Fjord of Norway to stimulate non-toxic algae [22,23]. During the experiment, a 390 kW air compressor was used to inject air continuously. The results showed that 88 m^3 deep sea water could be lifted from 40 m to 5–15 m with each air injection of 1 Nm^3 [10] and growth of phytoplankton was increased with a relative reduction of toxic algae. For these artificial upwelling technologies, using a mechanical pump and air pump to produce upwelling is the most stable and reliable method. However, the major obstacle is the high energy consumption.

The oligotrophic phenomenon in the water body of seaweed aquiculture will be alleviated by using artificial upwelling [24]. However, for the objective of enhancing the seaweed productivity in a large offshore aquaculture area, it is necessary to increase the amount of upwelling and achieve self-supplied energy. Therefore, large-scale artificial upwelling needs to be equipped with a large-scale offshore energy supply platform [25]. Optimizing the engineering parameters to decrease energy consumption and improve energy utilization efficiency are also key points to solve the energy problem of artificial upwelling technology in the future.

There are many developments in energy-saving technologies in various fields. Many control strategies are proposed for energy management of a hybrid energy system to achieve reasonable energy storage and utilization [26–28]. Moreover, in some smart and sustainable buildings [29], there will be an intelligent energy management system to save energy and control the indoor temperature and humidity. For the artificial upwelling, a control strategy to achieve energy management is also necessary. A carbon sequestration efficiency index is proposed by Pan et al., which is to indicate the effect of artificial upwelling with the power consumption [30]. However, few energy management strategies of artificial upwelling in engineering were found in literatures.

This paper focused on the development of energy management technology for air-lift artificial upwelling engineering by optimizing air injection. The engineering is to assist seaweed aquaculture for carbon sequestration. The mode and intensity of air injection are adjusted from the feedback of information on velocity variation in tidal currents, illumination, and temperature of the surface layer. The optimal operational planning is obtained by comparing the simulation results carried out by MATLAB. The experiments prove that, with the reasonable working time and air injection control, the nutrients of bottom water are lifted by artificial upwelling and crop yield is successfully increased.

The rest of the paper is organized as follows. Section 2 presents a system architecture of artificial upwelling platform, which provides the system components, mathematical representation, and the control strategy with a graphical user interface for the energy management. Section 3 shows the results obtained by simulation. Section 4 presents the experimental setup and results. Finally, the conclusion is given in Section 5.

2. System Architecture and Methodology

2.1. System Location and Architecture

The test location of ecological engineering for carbon sequestration is at 36°22′ north latitude and 120°50′ east longitude in AoShan Bay, Qingdao, China, as shown in Figure 1. The data of nutrient concentration around the location in March 2018 show that the surface seawater is nutrient-limited, the bottom water has more nutrients, and the sediments contain abundant nutrients in Table 1, so this area is not suitable for seaweed aquaculture. If there are artificial methods to change this situation, it is very beneficial to the development of the local economy, while air-lift artificial upwelling can lift bottom water with more nutrients so that it can change the status of lacking in nutrients in the surface water. This engineering is used to assist seaweed aquaculture and the object of cultivation is kelp, as a kind of seaweed whose area is about 48,000 m^2. The platform as shown in Figure 2 is far away from the land, so solar energy is used to achieve a self-powered supply. The electric energy is limited, so it is important to use it effectively, and the surface area of the platform is about 400 m^2 and the height is 26 m. There are 4 anchors, each with a mass of 3 tons, so that the platform will not move in the sea.

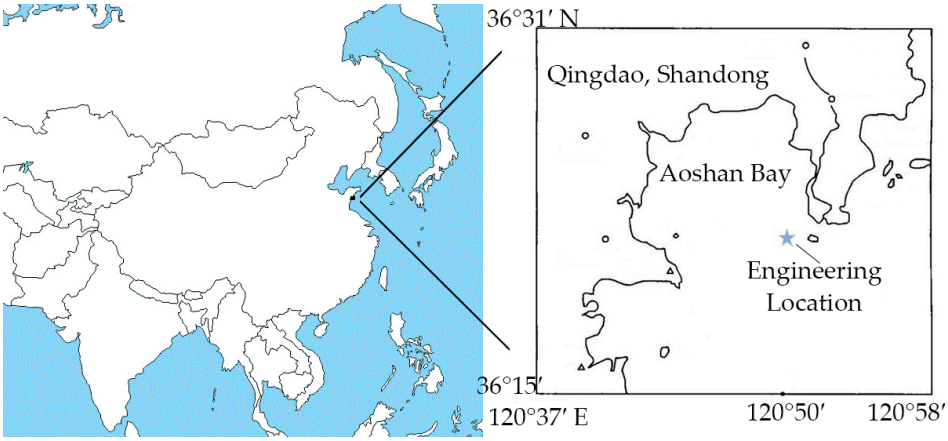

Figure 1. Test location of ecological engineering.

Table 1. The nutrients concentration of surface water, bottom water and sediments around the test location.

	Phosphorus (PO_4^-)	Nitrogen (NO_3^-+NO_2^-)
Surface water (umol/L)	0.30	8.31
Bottom water (umol/L)	0.20	10.65
Sediments (umol/L)	78.32	193.70

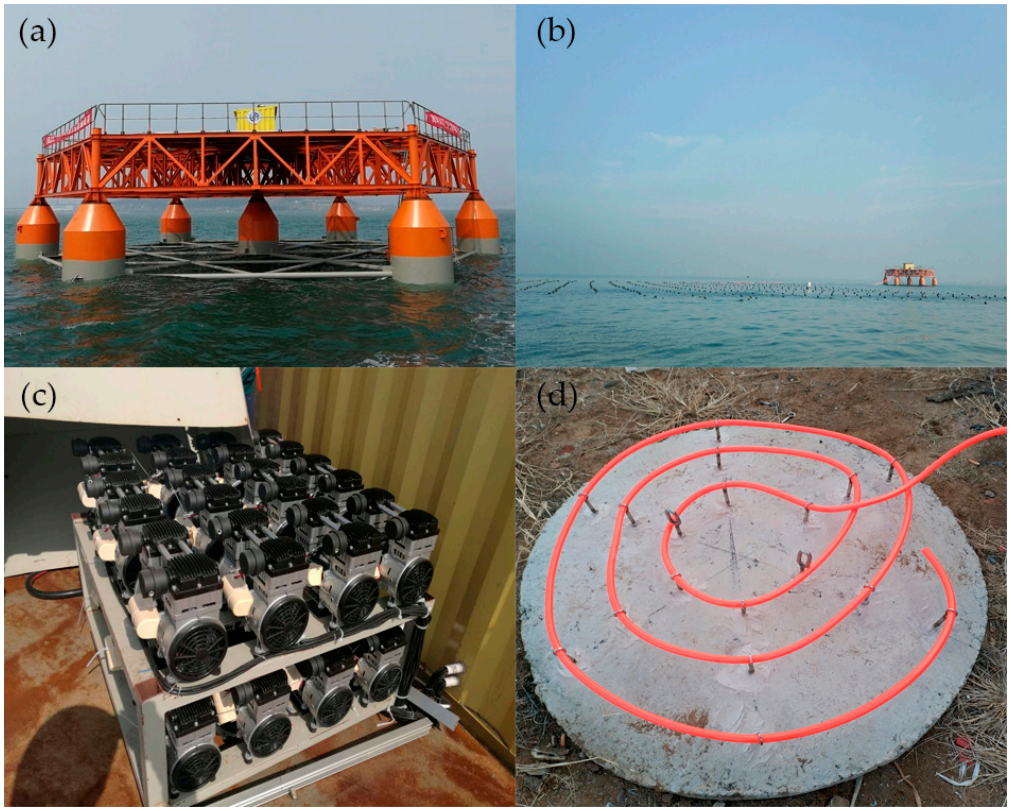

Figure 2. Picture of (**a**) artificial upwelling platform, (**b**) seaweed aquiculture, (**c**) air pumps, and (**d**) fixation for pipeline.

The platform consists of four systems: power system, sensor system, control system, and air injection system. The system architecture is shown in Figure 3. The hardware of the power system includes solar panels, batteries, and inverters. The total area of solar panels is about 240 m^2. The electric energy generated by solar panels is stored directly in the battery, and alternating current is generated through the inverter, which is 220 V and 50 Hz. Each battery is 12 V-150 Ah and the capacity is 1.8 kWh. The system can work for 0.9 h only on the battery when all air pumps are opened. Users can check the remaining energy and real-time output voltage and current in the inverter. The sensor system is used to measure ocean environment data, including temperature, illumination, and flow velocity, and then transmit these data directly to the control system. The control system uses Raspberry Pi as the central processing unit, which is a microcomputer. It receives and reads the data sent by sensors and controls the air injection system by a programmable logic controller (PLC). Raspberry Pi can also communicate with personal computers through a 4G network to achieve remote human intervention. The air injection system is composed of a number of air pumps, and the air pumps are connected with the air injection pipelines whose outer diameter is 16 mm and the thickness is 4 mm. The length of the pipelines is at least 150 m from the platform to the aquiculture area. The concrete block of about 60 kg is used as a fixation for an air injection nozzle, which is located on the seabed at a depth of 10 m in the aquiculture area. Nutrients lifted by upwelling will be directly used for kelp growth.

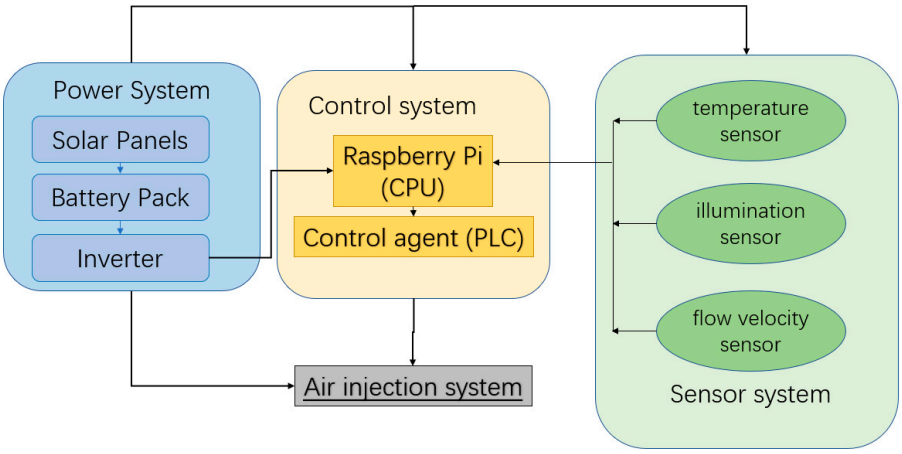

Figure 3. System Architecture. CPU: central processing unit; PLC: programmable logic controller.

2.2. Multilevel Control

The multilevel control system is more practical, efficient, and stable. The artificial upwelling system can also use a multilevel control. The system studied here consists of two layers: the supervisor controller and the local controller. The supervisor controller monitors and controls the electric energy output to power consumption centers, including the sensor system and the air injection system. At the same time, it checks the system for anomalies and errors. The local controller processes ocean environment parameters to control the air injection system to optimize air injection and improve efficiency. The local controller is limited to the supervisor controller. The control system aims to fulfill the following three goals:

1. Use electric energy rationally.
2. Ensure the security of the whole system.
3. Produce efficient upwelling and improve the efficiency of the system.
4. In the following subsections, these two control layers are described in detail.

2.2.1. Supervisor Controller

The supervisor controller is mainly to control electric energy. According to the residual power of the system and real-time voltage and current, charging of the battery and the energy supply of the sensor system and air injection system are controlled. If there are abnormalities and errors in the system, the controller will make an alarm, then cut off the power supply of the corresponding components. The user can receive the signal and deal with the situation. The control block diagram of the supervisory control layer is shown in Figure 4.

If the remaining energy is less than 10% of the full capacity, cut off the energy supply of other systems except the control system; if the remaining energy reaches the full capacity, shut down the battery charging; if the real-time output power is higher than 80% of the maximum output power, shut down the air injection system first, if it is still higher, then shut down the other systems. The management logic is shown below

$$\begin{cases} \begin{cases} If(W_r < 0.1W_0) \\ \rightarrow K_p = 0, K_s = 0, K_c = 1 \end{cases} \\ \begin{cases} If(W_r < W_0) \\ \rightarrow K_c = 1 \end{cases} \\ \begin{cases} If(W_r = W_0) \\ \rightarrow K_c = 0 \end{cases} \\ \begin{cases} If(P_o > 0.8P_{\max}) \\ \rightarrow K_p = 0, then \rightarrow K_s = 0 \end{cases} \end{cases} \quad (1)$$

In the above, W_r and W_0 are the remaining energy and full capacity, P_o and P_{max} are the real-time output power and maximum output power, where $P_o = U_{rt}I_{rt}$ and U_{rt}, I_{rt} are real-time voltage and current. W_r, U_{rt} and I_{rt} can be obtained by reading the inverters from the CPU and W_0, $P_{\max}$ are fixed values which depends on the system. K_p and K_s are the operation model (ON/OFF) of energy supply for the air injecting system and the sensor system, where ON is 1 and OFF is 0. K_c is the operation model (ON/OFF) of battery charging. When the battery is fully charged, K_c is OFF, which means there is no more charging for the battery. It is an overcharge protection.

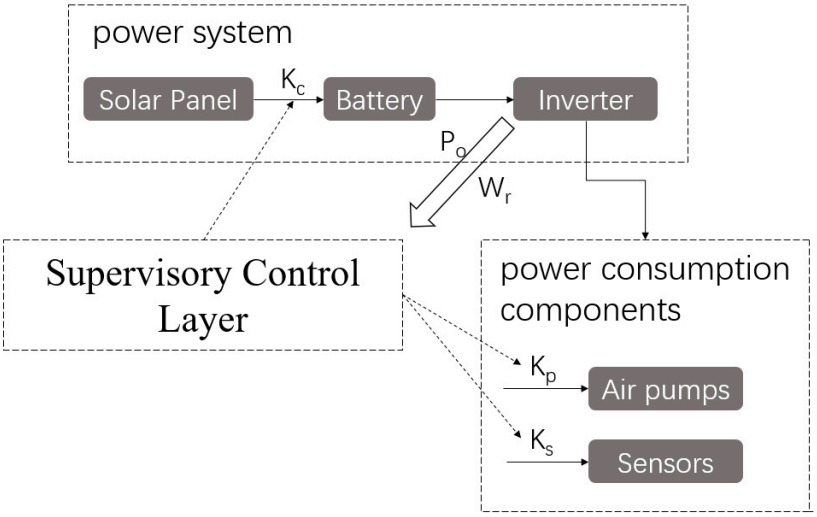

Figure 4. Control block diagram of supervisory control layer.

2.2.2. Local Controller

The local control system controls air injection according to the ocean environment. The parameters used to reflect the ocean environment include the flow velocity, illumination, and temperature. The flow velocity influences the height of upwelling plume and illumination and temperature influence the growth of kelp. The following sections will explain how the control system controls the air injection system according to the environmental parameters.

(1) Air injection rate calculation by flow velocity

The height of the upwelling plume is directly determined by the air injection rate and flow velocity. If the plume height cannot reach the kelp culture area, the upwelling is invalid. There has been some research on the behavior of plume in air-injection artificial upwelling [21,31,32]. Of the three variables, target height of plume, flow velocity, and air injection rate, any two variables are known and another variable can be obtained. In this controller, flow velocity, air injection rate and target height of upwelling are input, controlled quantity and output, respectively. However, the air injection rate is limited by the maximum output power, so it has a maximum value. In practice, to ensure that the upwelling reaches the target height, the air injection rate can be variational by flow velocity or a fixed value but cannot be higher than the maximum.

(2) Growth rate calculation by temperature and illumination

Temperature and illumination directly affect the photosynthesis and respiration of kelp, thus influencing the growth rate and nutrient uptake. When the growth rate is small and less nutrients are required, the lifted nutrients cannot be completely absorbed and will be waste. Temperature and illumination will be used to calculate the growth rate of kelp.

The net growth rate of kelp is determined by the difference between its total growth rate and respiration as [33]

$$N_{growth} = G_{growth} \times (1 - resp) \quad (2)$$

where N_{growth} is net growth rate, G_{growth} is total growth rate and *resp* is respiratory rate of kelp, which is influenced by temperature and can be determined by [34]

$$resp = \frac{0.3197 \times T^2 - 6.5728 \times T + 52.851}{100} \tag{3}$$

where T is measured temperature whose unit is °C. The total growth rate is influenced by temperature, illumination, and nutrient as [35]

$$G_{growth} = f(I) \times f(T) \times f(NP) \tag{4}$$

where G_{growth} is dimensionless. $f(I)$ is calculated by photoinhibition mode as [36]

$$f(I) = \frac{I}{I_s} \times \exp(1 - \frac{I}{I_s}) \tag{5}$$

where I is surface illumination, the unit is $umol \cdot m^{-2} \cdot s^{-1}$ and I_s is the optimum illumination for kelp and I_s= 180 $umol \cdot m^{-2} \cdot s^{-1}$. Compared with measured illumination, the underwater illumination has a certain attenuation. The optical attenuation coefficient of water can be expressed as [37]

$$K_d = 0.8813 + 0.0931 C_{ss} \tag{6}$$

where C_{ss} is suspended matter concentration and measured in local water, and the underwater illumination can be calculated by [38]

$$I(z) = I_0 e^{-K_d z} \tag{7}$$

where z is the depth from surface whose unit is m; $I(z)$ is the illumination at depth of z; I_0 is the illumination at surface, which is measured by sensor, whose unit is Lux. And $1000 Lux = 18 umol \cdot m^{-2} \cdot s^{-1}$. $f(T)$ is calculated as [36]

$$f(T) = \exp\left[-2.3 \times \left(\frac{T - T_{opt}}{T_x - T_{opt}}\right)^2\right] \tag{8}$$

in which T_{opt} is the optimum temperature for kelp growth, T_{opt}= 10 °C and T_x is temperature ecological amplitude. If $T \leq T_{opt}$, $T_x = T_{\min}$, or else $T_x = T_{\max}$. $T_{\min}$ and $T_{\max}$ are lower limit and upper limit of temperature ecological amplitude and $T_{\min} = 0.5$ °C, $T_{\max}$= 20 °C. The temperature, illumination, and flow velocity are obtained by corresponding sensors. $f(NP)$ is affected by ratio of nitrogen to phosphorus in kelp and its value is in (0,1]. When N:P of seawater is in [12,16], $f(NP)$= 1. When nitrogen or phosphorus is limited, $f(NP)$ can be obtained by a complex calculation which can refer to the research done by Wu [33].

(3) Air injection control with kelp growth model

The larger the growth rate of kelp, the larger the nutrient demand. The growth of kelp Z can be expressed as follows:

$$Z = \int_{t_1}^{t_2} N_{growth} dt \tag{9}$$

During this period, from t_1 to t_2, the energy consumption of the air injection system W can be expressed as:

$$W = \int_{t_1}^{t_2} P(t) dt \tag{10}$$

where $P(t)$ is consumption power of electric energy whose unit is watt and is determined by air injection rate as follows:

$$P(t) = (Q_0(t) + 58.691)/0.1045 \tag{11}$$

in which $Q_0(t)$ is air injection rate whose unit is L/min.

The solar system produces a certain amount of electrical energy every day. Most of the electrical energy will be used in the air injection system on that day, and the rest will be used to ensure the normal operation of other systems. Therefore, when kelp growth rate is large, using up the energy generated each day to produce upwelling is effective. Under this condition, making Z max with fixed W, the working time of the air injection system can be calculated, which is t_1, t_2 in formula (9) (10). This calculation is carried by MATLAB and only considers the continuous working once a day of the air injection system.

(4) Lifted nutrients calculation

The amount of lifted nutrients is an important measure to the efficiency of upwelling. In order to calculate the amount of lifted nutrients, the volume flux of upwelling needs to be known. This volume flux is also determined by air injection rate [31]. The expression is:

$$\frac{Q_w(z_\mathrm{h})}{Q_0} = 0.06{Q_0}^{-2/3}\left(\tanh\left(\frac{\sqrt[3]{gQ_0}}{H_0 \times 0.25}\right)\right)^{3/8}(\Delta z + z_h)^{5/3} \tag{12}$$

where z_h is the height from the bottom; Q_0 is the air injection rate determined by the opening of air pumps and its unit is m^3/s; $Q_w(z_\mathrm{h})$ is the initial volume flux at z_h; H_0 is head of the atmospheric pressure and is approximately equal to 10.4 m; Δz is offset of the nozzle origin, which can be determined as [31]

$$\Delta z = \frac{2b_0}{2.4 \times \alpha} \tag{13}$$

in which b_0 is nominal half-width of the plume near the nozzle; α is entrainment coefficient and $\alpha = 0.2$ here. The total amount of nutrients φ to be lifted can be expressed as

$$\varphi = \int\int Q_w(z) \cdot C_n(z) dz dt \tag{14}$$

where $C_n(z)$ is the concentration of nutrients at depth of z.

(5) Solar power generation calculation

According to design specifications of photovoltaic power station, a formula for calculating generating capacity can be expressed as [39]

$$Ep = \frac{HA \times PAZ \times K}{1000\mathrm{W/m}^2} \tag{15}$$

where Ep is the electric energy generation of a system whose unit is kW·h, HA is the daily total horizontal solar radiation and the unit is kW·h/m^2, PAZ is the system-installed capacity and the unit is kW, K is the correction factor, which depends on line loss, surface pollution, and angle of solar panels. K is determined by the theoretical and actual energy generation.

$$HA = GH \times 24 \tag{16}$$

where GH is averaged solar radiation, which can be obtained by the website of the local weather bureau and the unit is kW/m^2.

2.3. Graphical User Interface

For the artificial upwelling platform, a GUI is designed using MATLAB GUIDE to monitor energy consumption and system operation. Figure 5 shows an example of GUI. The GUI-based simulation platform allows users to set the parameters of the system and observe system performance.

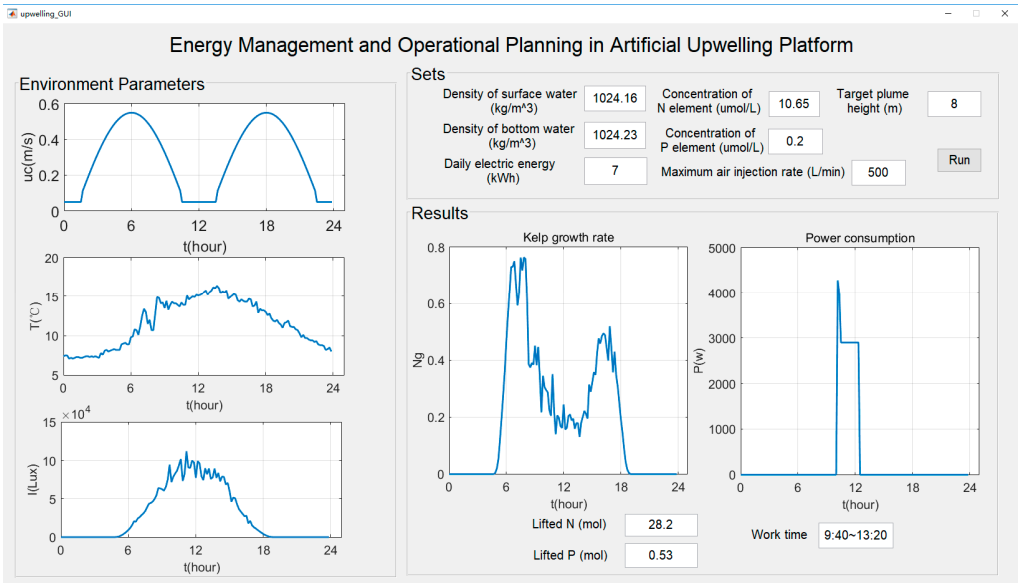

Figure 5. Graphical user interface based simulation platform for energy management and operational planning.

In the GUI, users can define several basic parameters, including "Density of surface water," "Density of bottom water," "Concentration of N, P element," "Target plume height," "Maximum air injection rate," and "Daily electric energy." Except "Maximum air injection rate," other parameters are changed, which should be measured regularly. "Target plume height" is the distance from kelp to seabed. After all user-defined parameters have been configured, users can press the "Run" button to start simulation. In the panel named "Environment Parameters," Flow velocity, temperature, and illumination are shown obtained by corresponding sensors. In the panel named "Results," users can observe the kelp growth rate and consumed power in work time, which can produce valid upwelling, and the results in text are one-day total including "Lifted N, P" and "Work time."

3. Simulation Setup and Results

3.1. Simulation Setup

The experimental environment of platform in AoShan Bay is considered in this section and its parameter values are shown in Table 2. The maximum output power of the energy system is 36 kW. For safety and consumption of other components, the power consumption for the air injection system should not exceed 30 kW and the total air injection rate Q_{tmax} should not exceed 3000 L/min. In order to expand the impact area and think about the actual aquaculture condition, the system has set up six groups of upwelling subsystems, each of which is the same. Therefore, the maximum air injection rate Q_{0max} of each group is 500 L/min. In the kelp aquaculture area, the water depth is 10 m and the target height of the upwelling plume H_0 is 8 m. The air injection pipelines are laid on the seabed with many small nozzles for air outlet. The total area of nozzles is equivalent to the circle whose diameter d_0 is about 80 cm. The density of the water around the air pipeline ρ_d is 1025.23 kg/m^3, and the concentrations of N (C_N) and P (C_P) nutrients here are 10.65 umol/L and 0.2 umol/L, respectively. The nutrient concentration is of the bottom water, while upwelling will disturb sediments and promote nutrients in sediments at the same time. Therefore, the actual lifted nutrients are much larger than the calculated value. The calculation of nutrients here only provides a reference for comparison. The density of surface water ρ_u is 1025.16 kg/m^3. The flow velocity shown in Figure 6 is simulated for the semi-diurnal tide. The flow velocity at 6 o'clock and 18 o'clock reaches the maximum. The temperature and illumination measured by sensors are also shown in Figure 6. The sampling interval is 10 min.

Table 2. Experimental environment parameter values in AoShan Bay.

Parameter	Q_{0max} (L/min)	H_0 (m)	C_{ss} (mg/L)	ρ_u (kg/m^3)	ρ_d (kg/m^3)	C_N $(umol/L)$	C_P $(umol/L)$	d_0 (m)
Value	500	8	15	1025.16	1025.23	10.65	0.2	0.8

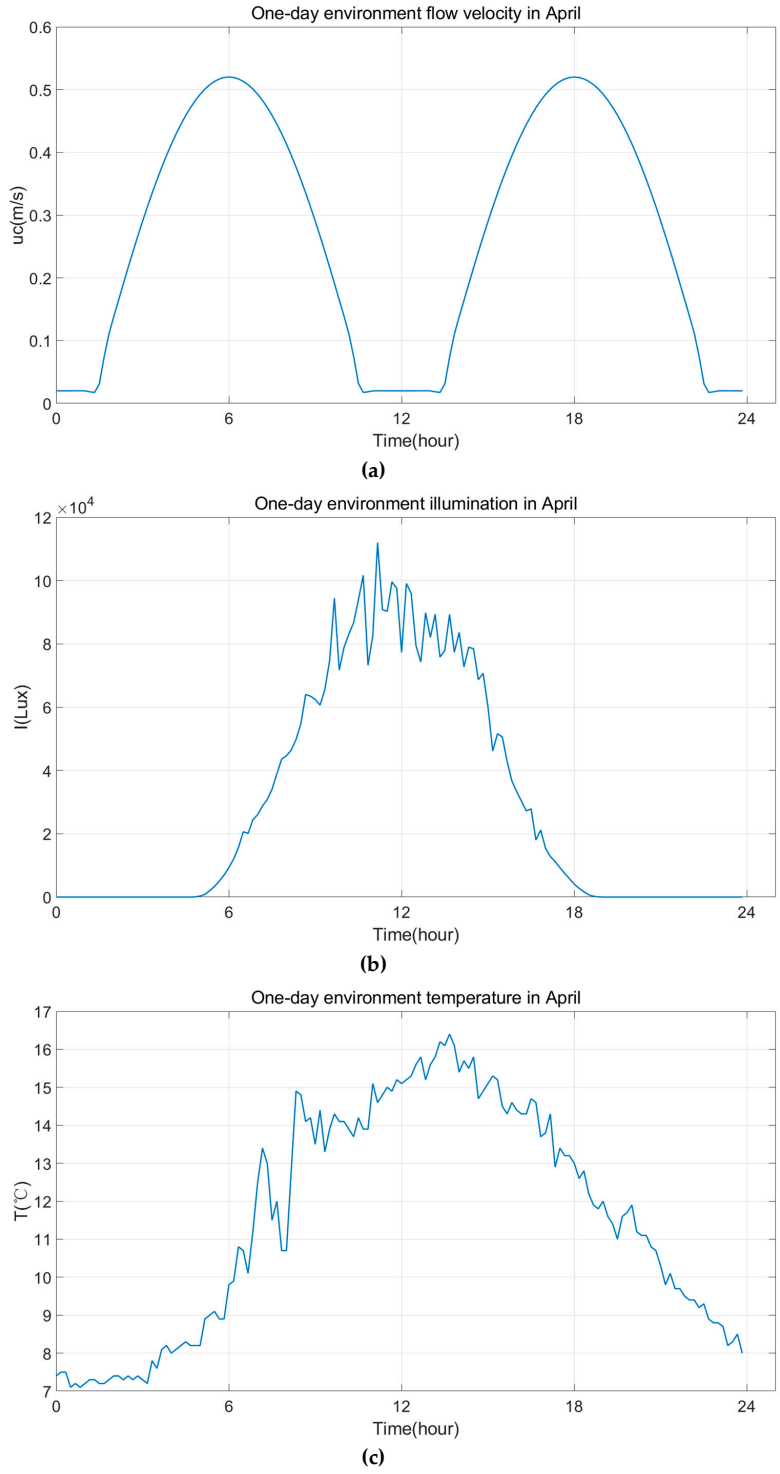

Figure 6. Environment parameters measured by sensors on a day in April including (**a**) The relationship between flow velocity and time; (**b**) The relationship between illumination and time; (**c**) The relationship between temperature and time.

3.2. Energy Generation

The total solar energy generation is determined by installed capacity and average radiation. The installed capacity is determined by the system itself. The system-installed capacity PAZ is 38.88 kW. The monthly average radiation and the daily average electric energy production per month calculated by the formula (15) are shown in Figure 7, and the correction factor K is 0.3. From April to August, the system generates more electric energy, about 48 kWh, while from December to January, it generates less, about 20 kWh due to the different solar radiation.

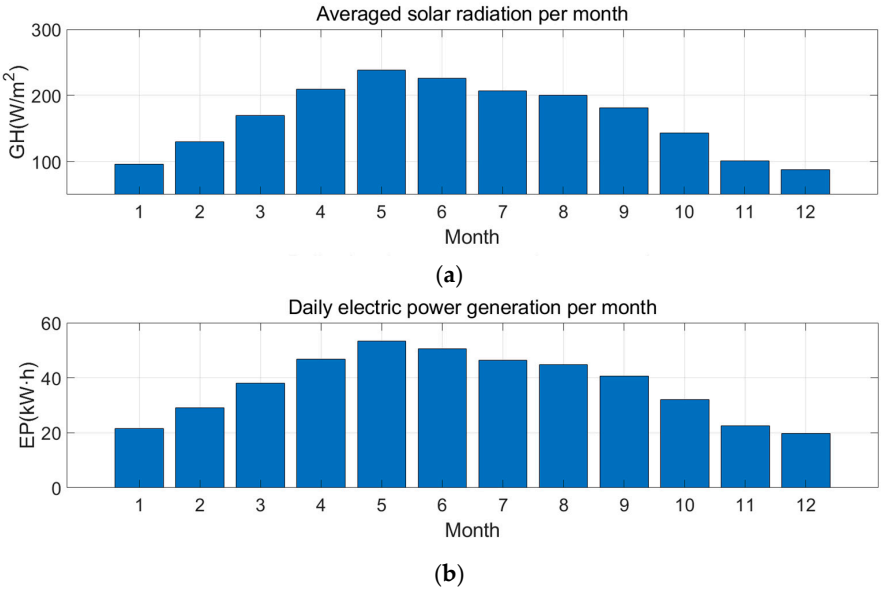

Figure 7. Energy generation of artificial upwelling platform: (**a**) Monthly average solar radiation in AoShan Bay; (**b**) Daily electric power generation per month of energy system.

3.3. The Relationship between Air Injection Rate and Flow Velocity

When the target height is 8 m, the relationship between air injection rate and flow velocity is shown in Figure 8. When the flow velocity is greater than 0.28 m/s, it takes more than 500 L/min air injection rate to raise the upwelling to the target height while the power required for air injection has exceeded the maximum power of the subsystem.

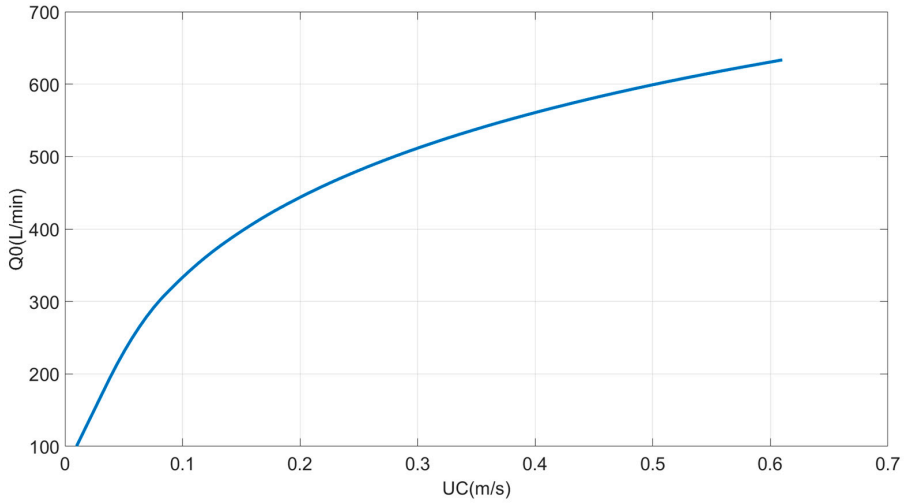

Figure 8. The relationship between air injection rate and flow velocity to make the upwelling reach the target height.

3.4. The Effect of Different Air Injection Modes

The subsection is divided into two parts for different air injection modes. In the first part, the air injection rate is fixed. In the second part, the air injection rate is variational and determined by flow velocity. The energy consumption and amount of lifted nutrients are compared.

3.4.1. Fixed Air Injection Rate

In this mode, the air injection rate is a fixed value, so the power consumption is also fixed. When the flow velocity is too large, the fixed air injection rate cannot lift the upwelling to the target height. In that time, the upwelling is invalid. When the flow velocity is very small, the upwelling height at fixed air injection rate can be larger than the target height and the upwelling is effective. The growth rate of kelp in a day is calculated according to the temperature and illumination conditions, as shown in Figure 9. According to Figure 6, the system can generate 46 kW·h electric energy a day. In order to ensure that other devices can work adequately, set up the air injection system to consume 42 kW·h a day, so there are 7 kW·h each day for subsystem. When the air injection rate is set to 160 L/min, the consumption power of the system is a fixed value, which is 2.093 kW. Therefore, the maximum opening time is 2.67 h. Affected by the flow velocity, when it is too big, the upwelling cannot be lifted to the specified height, then the air pumps will be closed. When the upwelling can be lifted to a target height, the pump is opened with 160 L/min air injection rate. The consumed power in a day is shown in Figure 10.

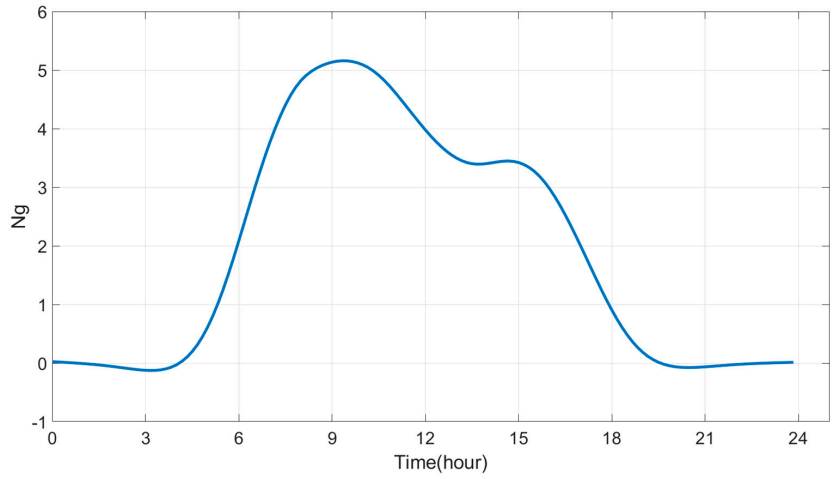

Figure 9. The growth rate of kelp in a day according to the temperature and illumination conditions.

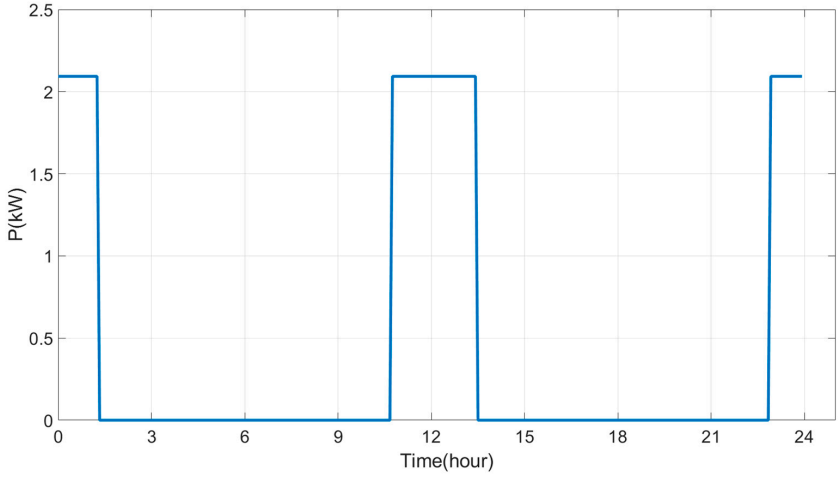

Figure 10. The consumed power for a day with given flow velocity when Q_0 = 160L/min.

Considering the nutrient utilization rate of kelp, when the growth rate of kelp is small, the rate of nutrient consumption is small. If there is upwelling, most nutrients will be wasted, so the air injection system will not work during this period. Therefore, when the air injection rate is 160 L/min, the optimum opening time of the air injection system is 10:45~13:25. The consumed energy is about 5.6 kW·h and the lifted N and P nutrients were 22.7 mol and 0.4 mol, respectively.

With different air injection rate and making sure that the upwelling can be lifted to target height, the working time of the air pump is different. The larger the air injection rate, the longer the working time. Because the consumed energy is limited and growth rate of kelp is variational, the optimum working time should be part of the working time. Using up the energy and lifting more nutrients will be best. By changing the fixed air injection rate, the optimal scheme and lifted nutrients of different air injection rates are shown in Table 3. The optimal scheme includes the choice of air injection rate and its optimum work time. The consumed energy and amount of lifted nutrients are indexes for evaluating upwelling.

Table 3. The optimal scheme and effect in different air injection rates.

Air Injection Rate (L/min)	Optimum Work Time	Work Duration (h)	Consumed energy (kW·h)	Lifted N/P (mol)
160	10:45–13.25	2.67	5.6	22.7/0.43
200	10:40–13:30	2.83	7	26.6/0.50
250	10:35–12:57	2.37	7	24.7/0.46
300	10:25–12:28	2.04	7	23.1/0.43
350	10:15–12:02	1.79	7	21.7/0.41
400	9:55–11:30	1.59	7	20.6/0.39
500	9:05–10:23	1.30	7	18.7/0.35

When the air injection rate is about 200 L/min, electric energy can be just used up, and the lifted nutrients are the largest.

3.4.2. Variational Air Injection Rate

Under this mode, the air injection rate can be changed, depending on the flow velocity, but not exceeding the maximum air injection rate of 500 L/min. The simulation is carried out under the same conditions as 3.4.1. When the upwelling can be lifted to a target height, the pump is opened with variational air injection rate. The consumed power in a day is shown in Figure 11.

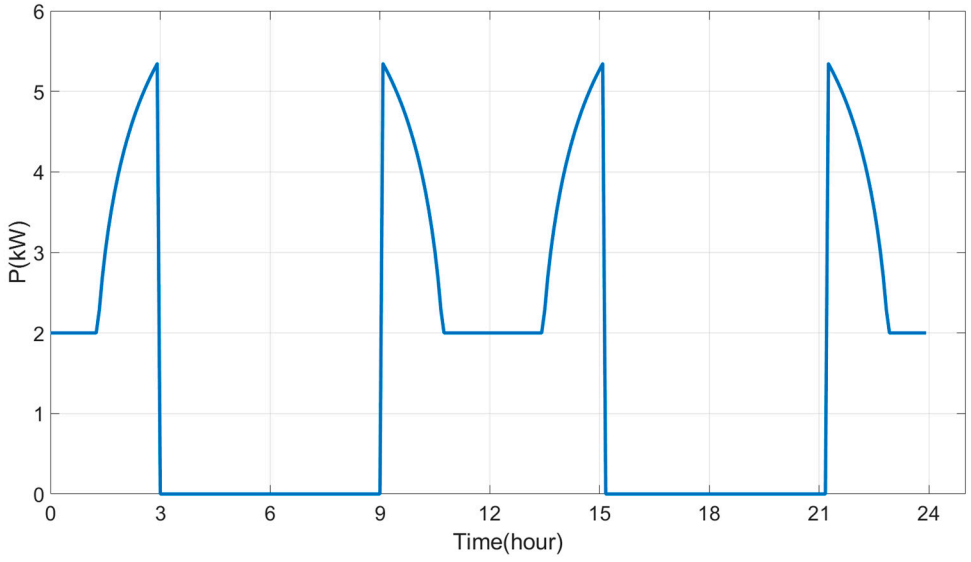

Figure 11. Consumed power for a day with variational air injection rate in the same situation.

According to the calculation method mentioned in formulas (9), (10), the optimum opening time is 10:15~13:25, and the energy consumption is about 7 kWh. The lifted N and P nutrients are 28.2 mol and 0.53 mol, respectively.

Comparing two air injection modes, the variable air injection rate is better. When the electric energy is used up, the amount of lifted nutrients can be the most. So, the energy efficiency is improved. Therefore, under the environmental conditions shown in Figure 6, the optimal scheme is to use variable air injection rate and the work time is 10:15~13:25.

4. Experiment Setup and Results

4.1. Experimental Setup

During the experiment in January 2019, data were measured around the air injection sea area when the system was working. The measured data included temperature, density, and dissolved oxygen, which were obtained by high-precision CTD (the conductivity-temperature-depth instrument, SBE 19plus V2). The nutrients are measured by sampling the seawater through a 5 L sampler. The background data is obtained in a nearby area without upwelling. The effect of upwelling was observed by comparing the data during the experiment with the background data.

The measurement stations for the experiment are shown in Figure 12. The coordinates of stations 1–10 are shown in Table 4. The point-solid line is the rope of kelp culture, the length of the rope is 120 m, and the interval between each rope is about 6 m. The position of the hollow circle in the figure is the upwelling area where the bubbles are produced and the solid circle is around at the location of air injection area. The direction of flow is almost parallel with the rope.

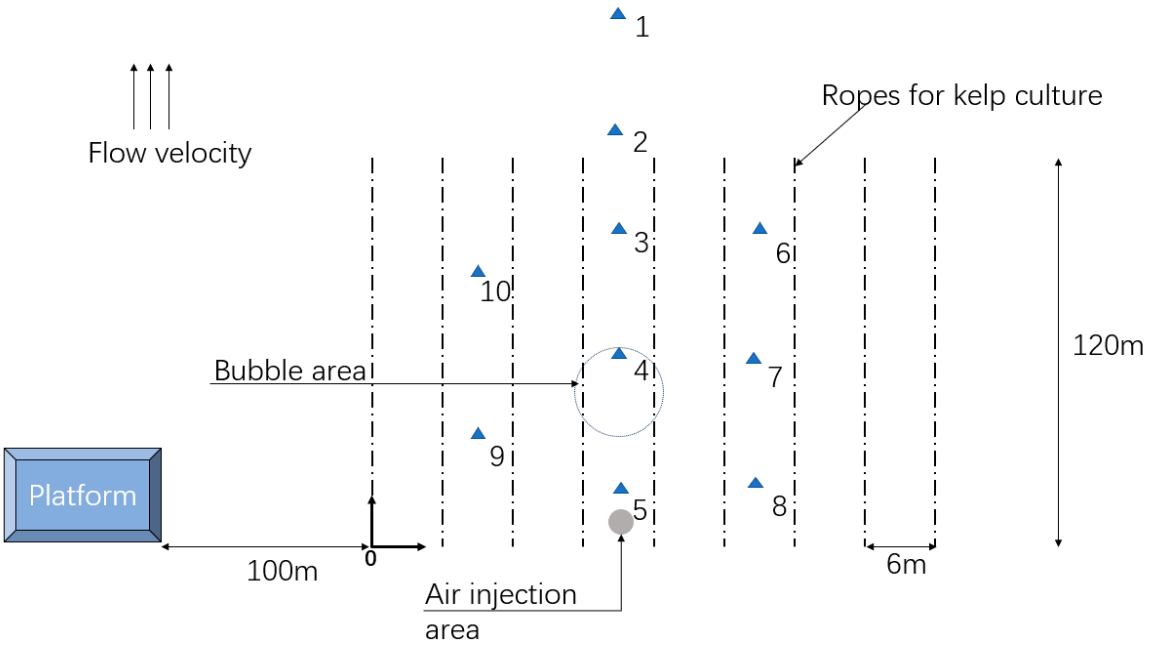

Figure 12. Measurement stations for artificial upwelling area.

Table 4. The coordinates of stations.

Stations	1	2	3	4	5	6	7	8	9	10
Coordinates (m)	(21,150)	(21,120)	(21,90)	(21,60)	(21,30)	(33,90)	(33,60)	(33,30)	(9,40)	(9,80)

In order to check the effect of the engineering, kelp sampling needs to be carried out. The experimental group of kelp is around the upwelling area and the control group growth in the nature environment without upwelling. At the time of sampling, the kelp had been growing for

three months. During this time, variable air injection was used to produce upwelling every day, which brings nutrients for the kelp in the experimental group. The measurement removes water from the surface of the kelp. There are 6 zones and 3 zones selected in the experimental group and control group, respectively. Ten kelp samples are obtained by random sampling in each zone.

4.2. The Validation of Upwelling

In this subsection, the performance of upwelling is presented. The bubbles of upwelling can be observed in the experiment as shown in Figure 13. The experimental data were processed and plotted as a curve of variable and depth. The results showed that the curve trend of stations 1, 6, 7, 8, 9, and 10 was not significantly different from the background value. The temperature of station 6 from 0 to 0.3 m underwater fluctuated slightly. The fitting results of temperature curves of stations 2, 3, 4, and 5 were shown in Figure 14. The temperature change reflects the location of the upwelling. Station 5 indicates that the upwelling is 2–4 m underwater and has not reached the surface of the water. Stations 3, 4 indicate that the upwelling has reached the surface of the water. Station 2 indicates that the bottom water brought by the upwelling has been fully mixed with the surface water, resulting in a declining temperature. The dissolved oxygen also increased in the surface, as shown in Figure 15. The measuring instrument CTD is of high precision, so the temperature and dissolved oxygen difference is not caused by system error. The results show that the artificial upwelling caused by the air injection does bring the bottom water to the surface and it is effective.

(a)

(b)

Figure 13. The pictures of air-lift upwelling and kelp culture: (**a**) Upwelling area where the bubbles are produced; (**b**) Picture of kelp culture area.

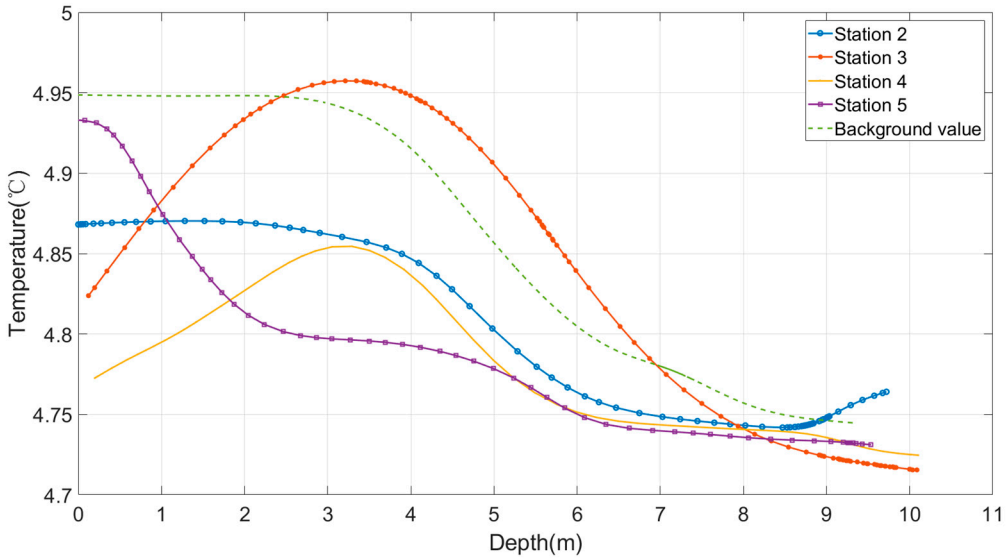

Figure 14. Comparison of the temperature profiles of stations 2, 3, 4, 5 with background value.

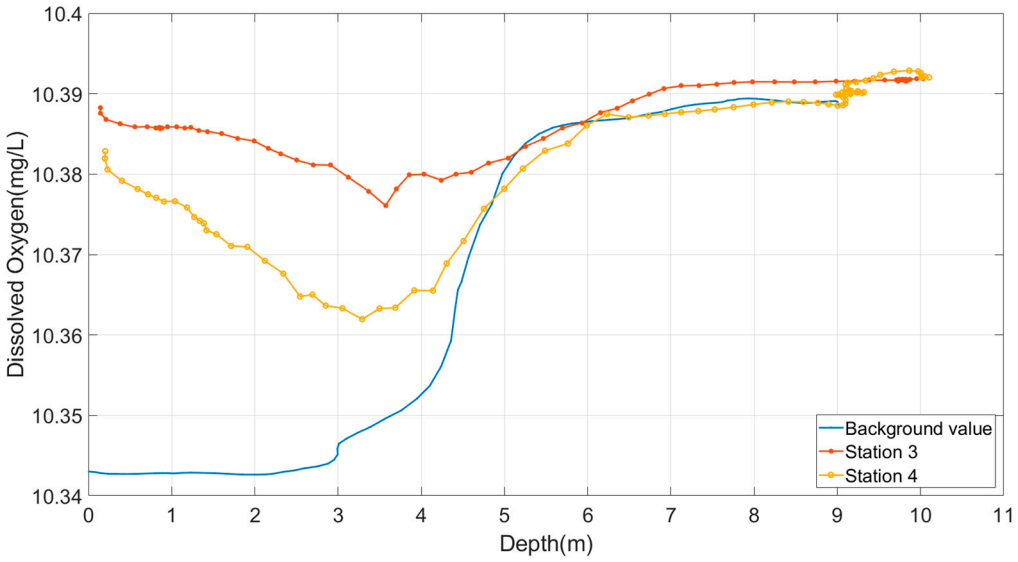

Figure 15. Comparison of the dissolved oxygen of stations 3, 4 with background value.

The data of concentration of nutrients $(NO_3^- + NO_2^-)$ in the samples are shown in Table 5. The samples of surface water were obtained when the system was working. The background value and experiment value are from the sample without and with upwelling, respectively. Comparing the background value, the concentration of experiment value increased. It proves that the upwelling has lifted the bottom water with more nutrients to the surface and improved the concentration, which is good for the growth of kelp.

Table 5. The concentration of nutrients $(NO_3^- + NO_2^-)$ in the surface water.

Station	NO_3^-+NO_2^-(*umol/L*)
1	4.768
2	4.67
3	4.944
4	4.806
Background value	4.23

4.3. The Effect of Engineering

The wet weight of kelp is shown in Table 6. The result is that the growth of kelp in the experimental group is better than that in the control group. The growing environments are the same, except that there is upwelling in the experimental group. With upwelling, there are more N, P nutrients for the growth of kelp. The result proves the effect of upwelling and the engineering of artificial upwelling increases the production of kelp for carbon sequestration.

Table 6. The wet weight of kelp with and without upwelling.

	Experimental Group				**Control Group**	
The wet weight of single kelp (g)	44	27.8	11.3	28.7	10.3	8.6
	37.6	66.3	15.8	12.6	12.5	8
	62.1	40.9	13.4	23.1	11	6.2
	44.1	46.8	13.1	22.4	8.2	6.1
	62.9	40.5	18.8	10.8	9.9	5.2
	63.2	71.7	16.9	56.8	17.7	12
	32	53.1	24.8	28.7	15.1	6.
	72	87.5	29.5	23	10	9
	79.8	36.8	19.5	14.8	13.8	7.4
	44.9	50.7	25	78.8	14.8	4.7
	34.6	32.3	25.6	14.6	7.7	6
	38.4	36.9	15.9	18.1	12.2	11
	19.1	42.9	8	10.3	14.3	10.2
	37.6	23.7	9.1	13.8	13.2	10
	24	32.5	21	11.1	12.6	9
Average (g)	33.1				10.1	

5. Conclusions

Reducing CO_2 emissions and increasing carbon storage is one of the greatest challenges in China for sustainable development of human society. The ecological engineering for carbon sequestration in coastal mariculture environments by using artificial upwelling has received increasing attention worldwide due to its potential positive environmental effects. However, the high energy consumption of the artificial upwelling is a barrier to implementation of the ecological engineering.

In the present work, the energy management strategy and operational planning of the ecological engineering were proposed to improve energy efficiency by optimizing the air injection mode. Its performance has been confirmed by the findings from the numerical simulations and field studies. Two modes of the new strategy (variable air injection rate) and the conventional one (fixed air injection rate) are compared in numerical simulations. Using variable air injection rate can lift more nitrogen nutrients of 28.2 mol than using fixed air injection rate of 26.6 mol, mostly with same energy cost. The field studies also validate the artificial upwelling by the profile of temperature and dissolved oxygen and the beneficial effect of engineering for the kelp growth. The results show that the new management strategy is feasible and effective in improving energy utilization efficiency of the ecological engineering. Sure, as a new and primitive management strategy, it still needs further improvement and perfection. The efficiency of the ecological engineering will increase in the future as the development of energy management technology for artificial upwelling. Wind power or wave power can be used in this engineering for more energy in the future. The presented new management strategy can also be easily adapted to other areas with similar characteristics and conditions, such as water delivery, aeration, and oxygenation.

Author Contributions: Conceptualization, W.F.; methodology, software, validation and writing—original draft preparation, T.L.; investigation, Z.Y., Z.Z. and R.Z.; writing—review and editing, C.X. and W.F.; supervision, W.F., Y.P. and Y.C.

Funding: This research was founded by the National Key Research and Development Program of China (No.2016YFA0601404) and the National Natural Science Funds of China (No. U1805242 and 41406084).

Conflicts of Interest: The authors declare no conflict of interest.

Nomenclature

α	entrainment coefficient $\alpha = 0.2$
b_0	nominal half-width of plume near the nozzle (m)
$C_n(z_\mathrm{h})$	concentration of nutrients at z_h
C_{ss}	suspended matter concentration $C_{ss} = 15mg/L$
g	gravitational acceleration $g = 9.8\mathrm{m/s}^2$
G_{growth}	total growth rate of kelp
H_0	head of the atmospheric pressure $H_0 = 10.4\mathrm{m}$
I	measured illumination (Lux)
$I(z)$	illumination at the depth of z (Lux)
I_0	illumination at surface (Lux)
I_s	optimum illumination for kelp I_s= 180 $umol \cdot m^{-2} \cdot s^{-1}$
I_{rt}	real-time current (A)
K_p	operation model (ON/OFF) of energy supply for air injection system
K_s	operation model (ON/OFF) of energy supply for sensor system
K_c	operation model (ON/OFF) of battery charging
K_d	optical attenuation coefficient of water (m^{-1})
N_{growth}	net growth rate of kelp
$P(t)$	power consumption at t
P_o	real-time output power
P_max	maximum output power
$Q_w(z_\mathrm{h})$	volume flux at z_h
Q_0	air injection rate (m^3/s)
$Q_0(t)$	air injection rate (L/min)
$resp$	respiration rate of kelp
t_1, t_2	work time of air injection system
T	measured temperature (°C)
T_x	temperature ecological amplitude (°C)
T_{opt}	optimum temperature for kelp T_{opt}= 10 °C
T_min	lower limit of temperature ecological amplitude $T_\mathrm{min} = 0.5$ °C
T_max	upper limit of temperature ecological amplitude T_max= 20 °C
U_{rt}	real-time voltage (V)
W	energy consumption (kWh)
W_r	remaining energy (kWh)
W_0	full charge capacity (kWh)
z	depth (m)
z_h	distance from the bottom (m)
Δz	offset of the nozzle (m)
Z	growth amount of kelp
φ	total amount of nutrients (mol)
Ep	electric power generation of system (kWh)
HA	daily total horizontal solar radiation (kWh/m^2)
PAZ	installed capacity $PAZ = 38.88\mathrm{k}W$
K	correction factor $K = 0.3$
GH	averaged solar radiation (kW/m^2)

References

1. Le Quéré, C.; Andres, R.J.; Boden, T.; Conway, T.; Houghton, R.A.; House, J.I.; Marland, G.; Peters, G.P.; Van der Werf, G.; Ahlström, A.; et al. The global carbon budget 1959–2011. *Earth Syst. Sci. Data* **2012**, *5*, 1107–1157. [CrossRef]
2. Zhang, Y.; Zhao, M.; Cui, Q.; Fan, W.; Qi, J.; Chen, Y.; Zhang, Y.; Gao, K.; Fan, J.; Wang, G.; et al. Processes of coastal ecosystem carbon sequestration and approaches for increasing carbon sink. *Sci. China Earth Sci.* **2017**, *60*, 809–820. [CrossRef]
3. Ianson, D.; Allen, S.E. A two-dimensional nitrogen and carbon flux model in a coastal upwelling region. *Glob. Biogeochem. Cycles* **2002**, 16. [CrossRef]
4. Smith, S.V. Marine macrophytes as a global carbon sink. *Science* **1981**, *211*, 838–840. [CrossRef] [PubMed]
5. Li, H.; Li, X.; Li, Q.; Liu, Y.; Song, J.; Zhang, Y. Environmental response to long-term mariculture activities in the Weihai coastal area, China. *Sci. Total Environ.* **2017**, *601*, 22–31. [CrossRef] [PubMed]
6. Lovelock, J.E.; Rapley, C.G. Ocean pipes could help the Earth to cure itself. *Nature* **2007**, *449*, 403. [CrossRef] [PubMed]
7. Williamson, P.; Wallace, D.W.; Law, C.S.; Boyd, P.W.; Collos, Y.; Croot, P.; Denman, K.; Riebesell, U.; Takeda, S.; Vivian, C. Ocean fertilization for geoengineering: A review of effectiveness, environmental impacts and emerging governance. *Proc. Saf. Environ. Prot.* **2012**, *90*, 475–488. [CrossRef]
8. Oschlies, A.; Pahlow, M.; Yool, A.; Matear, R.J. Climate engineering by artificial ocean upwelling: Channelling the sorcerer's apprentice. *Geophys. Res. Lett.* **2010**, *37*, L04701. [CrossRef]
9. Takahashi, T.; Sutherland, S.C.; Wanninkhof, R.; Sweeney, C.; Feely, R.A.; Chipman, D.W.; Hales, B.; Friederich, G.; Chavez, F.; Sabine, C.; et al. Climatological mean and decadal change in surface ocean pCO_2, and net sea–air CO_2 flux over the global oceans. *Deep Sea Res. Part Ii Top. Stud. Oceanogr.* **2009**, *56*, 554–577. [CrossRef]
10. Handå, A.; McClimans, T.A.; Reitan, K.I.; Knutsen, Ø.; Tangen, K.; Olsen, Y. Artificial upwelling to stimulate growth of non-toxic algae in a habitat for mussel farming. *Aquac. Res.* **2014**, *45*, 1798–1809. [CrossRef]
11. Masuda, T.; Furuya, K.; Kohashi, N.; Sato, M.; Takeda, S.; Uchiyama, M.; Horimoto, N.; Ishimaru, T. Lagrangian observation of phytoplankton dynamics at an artificially enriched subsurface water in Sagami Bay, Japan. *J. Oceanogr.* **2010**, *66*, 801–813. [CrossRef]
12. Pan, Y.; Wei, F.; Huang, T.H.; Wang, S.L.; Chen, C.T.A. Evaluation of the sinks and sources of atmospheric CO_2 by artificial upwelling. *Sci. Total Environ.* **2015**, *511*, 692–702. [CrossRef] [PubMed]
13. Ouchi, K.; Murphy, A.J. Real sea experiment of ocean nutrient enhancer "TAKUMI" upwelling deep ocean water. In Proceedings of the Oceans 2003. Celebrating the Past ... Teaming Toward the Future, San Diego, CA, USA, 22–26 September 2003.
14. Sato, T.; Tonoki, K.; Yoshikawa, T.; Tsuchiya, Y. Numerical and hydraulic simulations of the effect of Density Current Generator in a semi-enclosed tidal bay. *Coast. Eng.* **2006**, *53*, 49–64. [CrossRef]
15. Ouchi, K.; Yamatogi, T. A study on the entrainment with Density Current Generator. In Proceedings of the OCEANS 2000 MTS/IEEE Conference and Exhibition, Providence, RI, USA, 11–14 September 2000; pp. 787–790.
16. Zhang, X.; Maruyama, S.; Sakai, S.; Tsubaki, K.; Behnia, M. Flow prediction in upwelling deep seawater—The perpetual salt fountain. *Deep Sea Res. Part I Oceanogr. Res. Pap.* **2004**, *51*, 1145–1157. [CrossRef]
17. Fan, W.; Pan, Y.; Zhang, D.; Xu, C.; Qiang, Y.; Chen, Y. Experimental study on the performance of a wave pump for artificial upwelling. *Ocean Eng.* **2016**, *113*, 191–200. [CrossRef]
18. Kenyon, K.E. Upwelling by a wave pump. *J. Oceanogr.* **2007**, *63*, 327–331. [CrossRef]
19. Liu, C.C.; Jin, Q. Artificial upwelling in regular and random waves. *Ocean Eng.* **1995**, *22*, 337–350. [CrossRef]
20. Wei, F.; Chen, J.; Pan, Y.; Huang, H.; Chen, C.T.A.; Ying, C. Experimental study on the performance of an air-lift pump for artificial upwelling. *Ocean Eng.* **2013**, *59*, 47–57.
21. Liang, N.K.; Peng, H.K. A study of air-lift artificial upwelling. *Ocean Eng.* **2005**, *32*, 731–745. [CrossRef]
22. McClimans, T.; Handå, A.; Fredheim, A.; Lien, E.; Reitan, K.I. Controlled artificial upwelling in a fjord to stimulate non-toxic algae. *Aquac. Eng.* **2010**, *42*, 140–147. [CrossRef]
23. Aure, J.; Strand, Ø.; Erga, S.R.; Strohmeier, T. Primary production enhancement by artificial upwelling in a western Norwegian fjord. *Mar. Ecol. Prog. Ser.* **2007**, *352*, 39–52. [CrossRef]

24. Pan, Y.W.; Wei, F.; Zhang, D.H.; Chen, J.W.; Huang, H.C.; Liu, S.X.; Jiang, Z.P.; Yanan, D.I.; Tong, M.M.; Ying, C. Research progress in artificial upwelling and its potential environmental effects. *Sci. China Earth Sci.* **2016**, *59*, 236–248. [CrossRef]
25. Liang, N.K. Concept Design of Artificial Upwelling Induced by Natural Forces. In Proceedings of the OCEANS 91 Proceedings, Honolulu, HI, USA, 1–3 October 1991.
26. Aziz, A.S.; Tajuddin, M.F.N.; Adzman, M.R.; Ramli, M.A.; Mekhilef, S. Energy Management and Optimization of a PV/Diesel/Battery Hybrid Energy System Using a Combined Dispatch Strategy. *Sustainability* **2019**, *11*, 683. [CrossRef]
27. Trifkovic, M.; Sheikhzadeh, M.; Nigim, K.; Daoutidis, P. Modeling and Control of a Renewable Hybrid Energy System With Hydrogen Storage. *Ieee Trans. Control Syst. Technol.* **2013**, *22*, 169–179. [CrossRef]
28. Xie, S.; Hu, X.; Lang, K.; Qi, S.; Liu, T.J.S. Powering Mode-Integrated Energy Management Strategy for a Plug-In Hybrid Electric Truck with an Automatic Mechanical Transmission Based on Pontryagin's Minimum Principle. *Sustainability* **2018**, *10*, 3758. [CrossRef]
29. Wang, L.; Wang, Z.; Yang, R. Intelligent Multiagent Control System for Energy and Comfort Management in Smart and Sustainable Buildings. *Ieee Trans. Smart Grid* **2012**, *3*, 605–617. [CrossRef]
30. Pan, Y.; You, L.; Li, Y.; Fan, W.; Chen, C.-T.; Wang, B.-J.; Chen, Y. Achieving Highly Efficient Atmospheric CO2 Uptake by Artificial Upwelling. *Sustainability* **2018**, *10*, 664. [CrossRef]
31. Qiang, Y.; Fan, W.; Xiao, C.; Rivkin, R.B.; Pan, Y.; Wu, J.; Guo, J.; Chen, Y. Behaviors of Bubble-Entrained Plumes in Air-Injection Artificial Upwelling. *J. Hydraul. Eng.* **2018**, *144*, 4018032. [CrossRef]
32. Qiang, Y.; Fan, W.; Xiao, C.; Pan, Y.; Chen, Y. Effects of operating parameters and injection method on the performance of an artificial upwelling by using airlift pump. *Appl. Ocean Res.* **2018**, *78*, 212–222. [CrossRef]
33. Wu, R.; Zhang, X.; Zhu, M.; Zheng, Y. A model for the growth of Haidai (Laminaria japonica) in aquaculture. *Mar. Sci. Bull.* **2009**, *28*, 34–40.
34. Martins, I.; Marques, J.C. A Model for the Growth of Opportunistic Macroalgae (Enteromorpha sp.) in Tidal Estuaries. *Estuar. Coast. Shelf Sci.* **2002**, *55*, 247–257. [CrossRef]
35. Duarte, P. A mechanistic model of the effects of light and temperature on algal primary productivity. *Ecol. Model.* **1995**, *82*, 151–160. [CrossRef]
36. Zison, S.W.; Mills, W.B.; Deimer, D.; Chen, C.W. *Rates, Constants, and Kinetics Formulations in Surface Water Quality Modeling*, 2nd ed.; Environmental Protection Agency: Washington DC, USA, 1985; p. 455.
37. Zhang, Y.L. Regression analysis of beam attenuation coefficient under water in Lake Taihu. *Oceanol. Et Limnol. Sin.* **2004**, *35*, 209–213.
38. Kirk, J.T. *Light and Photosynthesis in Aquatic Ecosystems*; Cambridge University Press: Cambridge, UK, 1994.
39. GB50797-2012 Design Specification for Photovoltaic Power Station Design. Available online: https://wenku.baidu.com/view/12f0e391524de518964b7d9b.html (accessed on 4 June 2019).